Contents lists available at ScienceDirect

European Journal of Pharmaceutics and Biopharmaceutics

journal homepage: www.elsevier.com

Research paper

Progesterone lipid nanoparticles: Scaling up and in vivo human study

Elisabetta Esposito[a,*], Maddalena Sguizzato[a], Markus Drechsler[b], Paolo Mariani[c], Federica Carducci[c], Claudio Nastruzzi[a,*], Rita Cortesi[a]

[a] Department of Life Sciences and Biotechnology, University of Ferrara, I-44121 Ferrara, Italy
[b] BIMF/Soft Matter Electronmicroscopy, University of Bayreuth, Germany
[c] Department of Life and Environmental Sciences and CNISM, Università Politecnica delle Marche, I-60100 Ancona, Italy

ARTICLE INFO

Article history:
Received 19 July 2017
Received in revised form 27 July 2017
Accepted 27 July 2017
Available online xxx

Keywords:
Solid lipid nanoparticles
Nanostructured lipid carriers
Cryo-TEM
Tape-stripping
High-pressure homogenization

ABSTRACT

This investigation describes a scaling up study aimed at producing progesterone containing nanoparticles in a pilot scale. Particularly hot homogenization techniques based on ultrasound homogenization or high pressure homogenization have been employed to produce lipid nanoparticles constituted of tristearin or tristearin in association with caprylic-capric triglyceride. It was found that the high pressure homogenization method enabled to obtain nanoparticles without agglomerates and smaller mean diameters with respect to ultrasound homogenization method. X-ray characterization suggested a lamellar structural organization of both type of nanoparticles. Progesterone encapsulation efficiency was almost 100% in the case of high pressure homogenization method. Shelf life study indicated a double fold stability of progesterone when encapsulated in nanoparticles produced by the high pressure homogenization method. Dialysis and Franz cell methods were performed to mimic subcutaneous and skin administration. Nanoparticles constituted of tristearin in mixture with caprylic/capric triglyceride display a slower release of progesterone with respect to nanoparticles constituted of pure tristearin. Franz cell evidenced a higher progesterone skin uptake in the case of pure tristearin nanoparticles. A human in vivo study, based on tape stripping, was conducted to investigate the performance of nanoparticles as progesterone skin delivery systems. Tape stripping results indicated a decrease of progesterone concentration in *stratum corneum* within six hours, suggesting an interaction between nanoparticle material and skin lipids.

1. Introduction

Recent research efforts have demonstrated that nanotechnology achieves dramatic results in different scientific area, including drug formulation and delivery. Particularly, the advantages of lipid based nanoparticles, over conventional formulations, include: (a) the control of drug release and/or drug targeting; (b) the reduction of toxicity problems thanks to the use of biocompatible excipients (i.e. lipids) and avoidance of organic solvents, (c) the reduction of number of administrations and drug dosage, (d) the ability to solubilize poorly water-soluble drugs and finally (e) the vast range of administration routes [1–4].

For instance, the variation of lipid composition offers the possibility to produce nanoparticles with different properties; the use of lipids that are solid at room temperature, such as glyceryl tristearate results in the formation of the so called "solid lipid nanoparticles" (SLN), while employing mixtures of solid and liquid lipids results in the obtainment of nanostructured lipid carriers (NLC). NLC can be considered as second generation of SLN, in which the presence of liquid regions (within the nanoparticle matrix) increases the ability to solubilize lipophilic drugs and prevents drug leakage during storage [5,6].

Hot homogenization technique is by far the most widely used nanoparticle production approach; the method is based on dispersion of a melted lipid phase in a hot aqueous surfactant solution under stirring by high-shear mixing device. The obtained emulsion is then submitted to hot homogenization and cooling, finally obtaining nanoparticles by re-crystallization of lipids [7,8].

The homogenization step is mandatory to reduce size of droplets constituting the inner oil phase of the initial emulsion. The homogenization can be achieved by ultrasound, or by high pressure. Ultrasound homogenization (UH) is based on the transmission of high power ultrasound waves in a liquid media by a probe. Ultrasound waves generate small vacuum bubbles which implodes, resulting into high shear forces [9]. On the one hand, an important advantage of this

Abbreviations: SLN, solid lipid nanoparticles; NLC, nanostructured lipid carriers; PRG, progesterone; x-gum, xanthan gum; UH, ultrasound homogenization; HPH, high pressure homogenization; cryo-TEM, cryogenic transmission electron microscopy; PCS, photon correlation spectroscopy; EE, encapsulation efficiency; LC, loading capacity

* Corresponding authors at: Department of Life Sciences and Biotechnology, Via Fossato di Mortara, 19, I-44121 Ferrara, Italy.
Email addresses: ese@unife.it (E. Esposito); nas@unife.it (C. Nastruzzi)

http://dx.doi.org/10.1016/j.ejpb.2017.07.015
0939-6411/

method is low cost of instrumentation, on the other a drawback is formation of lipid agglomerates during cooling.

High pressure homogenization (HPH) is an ongoing process widely used in pharmaceutical and food industry, based on reduction of droplet/particle size and uniformity under conditions of extreme pressure by a piston-gap homogenizer. To produce lipid nanoparticles, the initial coarse emulsion is forced through a special homogenization valve at extremely high pressures (up to 150 MPa), at temperatures above the lipid melting point, leading to a secondary thin emulsion. Several homogenization cycles can be performed at 50–150 MPa, enabling to obtain lipid nanoparticles free from agglomerates. Notwithstanding its high cost, high-pressure homogenizer lab-scale and pilot-scale models can operate with limited sample volumes and produce the same results as large models, ensuring scalability of results. Thus, HPH enables to scale-up nanoparticle volume from lab to pilot and industrial scale [10,11].

Progesterone (PRG) is a steroid hormone present in different medicines with various indications such as the control of habitual abortion, suppression and synchronization of oestrus, regulation of ovulation and menstruation (e.g. to treat amenhorrea), treatment of infertility by luteal phase support and pevention of endometrial hyperplasia [12,13]. For these applications, PRG is typically administered orally, rectally, intramuscularly, subcutaneously or intravaginally [12,13].

Subcutaneous or intravaginal administered formulations for PRG are also commercially available; such medicines were designed to avoid first-pass metabolism, observed in the case of oral administration, to achieve higher concentrations.

Further formulations for PRG include those applied on the skin to treat deficiency associated with menopause and perimenopause, mastodynia or diffuse fibrocystic mastopathy.

In addition, PRG is present in cutaneous formulations (i.e. gels and creams) to treat dermatological disorders such as acne and ageing [14,15].

Regarding the pharmaceutical application of lipid nanoparticle, no formulations are on the market up to now, even though research studies have demonstrated that both SLN and NLC are suitable for many administration ways, including subcutaneous, vaginal and skin application [1,7]. Specifically, SLN and NLC are proposed for mucosal and skin applications, since they are non-irritant and non-toxic [6,10]. In this respect, the current study describes the encapsulation of PRG in SLN and NLC produced by UH and HPH methods. The obtained nanoparticle suspensions have been further formulated in viscous gels obtained by xanthan gum (x-gum) addition. Tape stripping experiments have been conducted to compare the performances of SLN and NLC gels applied on skin. Particularly PRG amount in *stratum corneum* has been evaluated after cutaneous application of the different nanoparticulate gels.

2. Materials and methods

2.1. Materials

The copolymer poly (ethylene oxide) (a) –poly (propylene oxide) (b) (a = 80, b = 27) (poloxamer 188) was a gift of BASF Chem-Trade GmbH (Burgbernheim, Germany). Miglyol 812 N, caprylic/capric triglycerides (miglyol) was a gift of Cremer Oleo Division (Witten, Germany). Tristearin, stearic triglyceride (tristearin), progesterone (PRG) and HPLC solvents were purchased from Sigma-Aldrich, Merck (Darmstadt, Germany).

2.2. Preparation of lipid nanoparticles

Lipid nanoparticles were alternatively prepared by hot homogenization techniques based on ultrasound or high pressure. In both cases the lipid phase (5% with respect to the whole weight of the dispersion) was constituted of pure tristearin (in the case of SLN preparation) or a mixture of tristearin and miglyol in a 2:1, w/w ratio (in the case of NLC preparation), while the aqueous phase was a poloxamer 188 solution (2.5, % w/w).

2.2.1. Ultrasound homogenization (UH) method

As first step an emulsion was obtained by addition of the aqueous phase (4.75 ml) heated at 80 °C to the molten lipid phase (250 mg) followed by mixing at 15,000 rpm, 80 °C for 1, 2 or 3 min (IKA T25 digital ultra-turrax) (data in brief, Fig. S 1A). As second step, the emulsion was subjected to ultrasound homogenization at 6.75 kHz for 5, 10 or 15 min (Microson ultrasonic Cell Disruptor-XL Minisonix) (data in brief, Fig. S 1B) and let cooling at 25 °C. Lipid nanoparticle dispersions were stored at room temperature.

2.2.2. High pressure homogenization (HPH) method

As first step, the aqueous phase (950 ml) heated at 80 °C was added to the molten lipid phase (50 g) and subjected to stirring at 15,000 rpm, 80 °C for 1, 2 or 3 min (data in brief, Fig. S 1C). The emulsion was homogenized using high pressure homogenizer for 1–3 cycles at 100 MPa (Panda Plus2000/GEA Niro Soavi, Parma, Italy) to form o/w nanoemulsion (data in brief, Fig. S 1D). The nanoemulsion was then cooled by a coil employed as heat exchanger directly connected to the instrument for solidification and formation of lipid nanoparticles. Lipid nanoparticle dispersions were stored at room temperature.

Both for UH and HPH methods, in the case of PRG loaded nanoparticles (named SLN-PRG and NLC-PRG), the drug (0.1%, w/w with respect to the whole dispersion; 0.02%, w/w with respect to the lipid phase) was added to the fused lipid phase before emulsification step.

2.3. Photon correlation spectroscopy (PCS) analysis

Submicron particle size analysis was performed using a Zetasizer 3000 PCS (Malvern Instr., Malvern, England) equipped with a 5-mW helium neon laser with a wavelength output of 633 nm. Glassware was cleaned of dust by washing with detergent and rinsing twice with water for injections. Measurements were made in triplicate at 25 °C at an angle of 90°, periodically from 0 to 6 months after nanoparticle production. Data were interpreted using the "CONTIN" method [16].

2.4. Cryogenic transmission electron microscopy (cryo-TEM) analysis

Samples were vitrified as previously described [17]. The vitrified specimen was transferred to a Zeiss EM922Omega transmission electron microscope for imaging using a cryoholder (CT3500, Gatan). The temperature of the sample was kept below −175 °C throughout the examination. Specimens were examined with doses of about 1000–2000 e/nm^2 at 200 kV. Images were recorded digitally by a CCD camera (Ultrascan 1000, Gatan) using an image processing system (GMS 1.9 software, Gatan). In addition, size distribution of nanoparticles was performed by measuring 1000 nanoparticles for each cryo-TEM image by the digital analyzer ImageJ 1.48v.

2.5. X-ray diffraction measurements

X-ray diffraction experiments were performed using a 3.5 kW Philips PW 1830 X-ray generator (Amsterdam, Netherlands) equipped with a Guinier-type focusing camera (homemade design and construction, Ancona, Italy) operating with a bent quartz crystal monochromator (λ = 1.54 Å). Diffraction patterns were recorded on GNR Analytical Instruments Imaging Plate system (Novara, Italy). Samples were held in a tight vacuum cylindrical cell provided with thin mylar windows. Diffraction data were collected at 37 °C. In each experiment, Bragg peaks were detected. The few peaks in the low-angle region were indexed considering the different symmetries commonly observed in lipidic phases [18] and the unit cell dimension of the phase, a, calculated from the averaged spacing of the observed peaks. Peaks in the wide-angle X-ray scattering region relate to the lateral organization of the hydrocarbon chains: from their positions, the subcell structure of the nanoparticles was determined.

2.6. Encapsulation efficiency and loading capacity of lipid nanoparticles

The encapsulation efficiency (EE) and loading capacity (LC) of PRG in SLN and NLC were determined as previously described [19]. 500 µl aliquot of each SLN and NLC batch was loaded in a centrifugal filter (Microcon centrifugal filter unit YM-10 membrane, NMWCO 10 kDa, Sigma Aldrich, St Louis, MO, USA) and centrifuged (Spectrafuge™ 24D Digital Microcentrifuge, Woodbridge NJ, USA) at 8000 rpm for 20 min. The amount of drug was determined after dissolving the lipid phase with a known amount of methanol (1:10, v/v) for 2 h under stirring. PRG content was analyzed after filtration by high performance liquid chromatography (HPLC) using an Agilent Zorbax Eclipse XBD-C18 column (Agilent Technologies, United States) (15 cm × 0.46 cm) stainless steel packed with 5 µm particles, eluted at room temperature with different mobile phases. Samples of 50 µl were injected through the rheodyne injector system fitted with 50 µl fixed loop and compared with standards of known concentration. The mobile phase composition was methanol/water (80:20, v/v), with flow rate 1 ml/min at 220 nm. Analyses were conducted in triplicate. EE and LC were determined following Eqs. (1) and (2), respectively.

$$EE = L\ /T \times 100 \quad (1)$$

$$LC = L\ /T_{\text{lipid phase}} \times 100 \quad (2)$$

where in Eq. (1) L is the amount of drug effectively present in the nanoparticles, T stands for the total amount of drug initially added to the lipid phase; in Eq. (2), L is the amount of drug effectively present in the nanoparticles, $T_{\text{lipid phase}}$ is the total weight of lipid phase in the formulation. Determinations were performed six times in independent experiments and the mean values ± standard deviations were calculated.

2.7. Prediction of long-term stability

The stability of PRG was assessed in SLN-PRG and NLC-PRG produced by UH or HPH methods and stored in glass containers at 25 °C for 6 months.

Chemical stability was evaluated, determining PRG content by HPLC analyses. Shelf life values were calculated as below reported [20].

Log (PRG residual content, %) was plotted against time and the slopes (m) were calculated by linear regression.

The slopes (m) were then substituted into the following equation for the determination of k values:

$$k = m \times 2.303 \quad (3)$$

Shelf life values (the time for 10% loss, t_{90}) and half-life (the time for 50% loss, $t_{1/2}$) were then calculated by the following equations:

$$t_{90} = 0.105/k \quad (4)$$

$$t_{1/2} = 0.693/k \quad (5)$$

2.8. In vitro PRG release studies

In vitro dialysis release studies were performed on PRG alternatively solubilized in SLN-PRG, NLC-PRG or suspended in poloxamer 188 solution (2.5%, w/w). Two milliliters of solution/suspension (PRG 0.1%, w/w) were put into a dialysis tube (6 cm) (molecular weight cut off 10,000–12,000; Medi Cell International, England), then placed into 30 ml of receiving phase constituted of phosphate buffer (10 mM, pH 7.4) and ethanol (70:30, v/v) and shaken in a horizontal shaker (MS1, Minishaker, IKA) at 175 rpm at 37 °C. Samples of receiving phase were withdrawn at regular time intervals, and analyzed by HPLC method as described above. Fresh receiving mixture was added to maintain constant volume. The PRG concentrations were determined six times in independent experiments and the mean values ± standard deviations were calculated.

2.9. Drug release data analysis

The experimental data obtained by the release experiments were fitted to the following semi-empirical equations respectively describing Fickian dissolutive (6) and diffusion (7) release mechanisms [21,22]

$$Mt\ /\ M\infty = K_{Diss}t^{0.5} + c \quad (6)$$

$$1 - Mt/\ M\infty = e^{-Kdiff}t + c \quad (7)$$

where $Mt/M\infty$ is the drug fraction released at the time t, ($M\infty$ is the total drug content in the analyzed amount of SLN or NLC), K and c are coefficients calculated by plotting the linear forms of the indicated equations. The release data of percentage of released drug (0–8 h) were used to produce theoretical release curves.

2.10. Gel production

SLN and NLC viscosity has been improved by adding x-gum (1%, w/w) directly into the dispersion and by slowly stirring for 1 h followed by hand mixing, until complete dispersion of the gum. The obtained viscous nanoparticle formulations have been named SLN-PRG/G and NLC-PRG/G.

2.11. In vitro skin permeation study

Samples of adult human skin (mean age 36 ± 8 years) were obtained from breast reduction operations. Subcutaneous fat was carefully trimmed and the skin was immersed in distilled water at 60 ± 1 °C for 2 min, after which SCE (*stratum corneum*/epidermis) was removed from the dermis using a dull scalpel blade. SCE membranes were dried in a desiccator at ~25% relative humidity. The dried samples were wrapped in aluminum foil and stored at 4 ± 1 °C until use.

SCE were then rehydrated by immersion in distilled water at room temperature for 1 h, before being mounted in Franz-type diffusion cells supplied by LGA (Berkeley, CA), as reported by Puglia and colleagues [23].

The exposed skin surface area was 0.78 cm^2 area (1 cm diameter orifice). The receptor compartment contained 5 ml phosphate buffer 10 mM pH 7.4 and ethanol (50:50, v/v), to allow the establishment of the sink conditions and to sustain permeant solubilization. This solution was stirred with the help of a magnetic bar at 500 rpm and thermostated at 32 ± 1 °C during all the experiments [24].

One gram of SLN-PRG/G or NLC-PRG/G was placed on the skin surface in the donor compartment and the latter was sealed to avoid evaporation. At predetermined time intervals comprised between 1 and 24 h, samples (0.15 ml) of receptor phase solution were withdrawn, PRG concentration in the receptor phase was measured using HPLC (as described in Section 2.6). Each removed sample was replaced with an equal volume of simple receptor phase.

After 6 and 24 h of permeation studies, to determine skin uptake, SCE portions (4.52 cm^2 area) were removed from the diffusion cell, rinsed with water and immersed in 5 ml of methanol, homogenized in vortex for 2 min, filtered by nylon membranes (200 nm diameter pores) and analyzed by HPLC.

The data were analyzed using Student's *t*-test, considering $p < 0.05$ as the minimum level of significance.

2.12. Tape stripping

In vivo experiments were conducted in accordance with The Code of Ethics of the World Medical Association (Helsinki Declaration 1964) and its later amendments for experiments involving humans and was approved by the Ethics Committee of the University of Ferrara, Italy (study number: 161,087). The volunteers were of both sexes in the age range 25–55 years and recruited after medical screening, including the filling of a health questionnaire followed by physical examination of the application sites. Informed consent was obtained from all individual participants included in the study. The participants did not suffer from any ailment and were not on any medication at the time of the study. They were rested for 15 min prior to the experiments and room conditions were set at 22 ± 2 °C and 40–50% relative humidity. For each volunteer, six sites on the ventral surface of forearms were defined using a rectangular template (2 cm^2) and marked with permanent ink. Three sites were treated with 200 mg of SLN-PRG/G and three with 200 mg of NLC-PRG/G. The preparations were spread uniformly by means of a plastic spatula and then the sites were occluded for 6 h. After the occlusion period, the residual formulations were removed by gently wiping with clean cotton balls.

Eleven individual 2 cm^2 squares of adhesive tape (Scotch Book Tape 845, 3M) were utilized to sequentially tape-strip the *stratum corneum* on the application sites. The first tape strip was discarded and not analyzed, since it may still contain some formulation residue not removed by the skin cleaning. The *stratum corneum* was collected in the treated sites at 1 h (t 1), 3 h (t 3) and 6 h (t 6) from the formulation removal [26]. The presence of *stratum corneum* on the adhesive tapes was routinely checked by light microscopy using a Nikon E800, 40× magnification (data in brief, Fig. S 2).

After stripping, all tapes from the same site were placed in a vial containing 2 ml of the HPLC mobile phase methanol:water (80:20 v/v) and vortexed for 1 min. The PRG present in the samples was then quantified by HPLC, as previously described in Section 2.6. The amount of PRG found in *stratum corneum* was plotted versus time and the area under the curve (AUC) was computed using the trapezoidal rule for comparison purposes. In vivo data are expressed as mean ± SD. Data obtained from the various formulations were compared by Student's *t* test. The employed software was Prism 5.0, Graph Pad Software Inc. (La Jolla, CA -304 USA), $p < 0.05$ was considered the minimum level of significance.

3. Results

3.1. Effect of experimental set up on lipid nanoparticles

Most of the experimental procedures for the preparation of lipid nanoparticles intended as solid lipid nanoparticles (SLN) or nanostructured lipid carriers (NLC) are characterized by small amount of lipid (80–250 mg) dispersed in a 5–50 ml water phase [17,27,28].

The main aim of the current paper is the development and analysis of a production protocol able to result in pilot scale batches of SLN and NLC.

HPH method indeed was compared with UH protocol, that was previously studied by our research group [17,29–32].

Therefore, SLN and NLC have been prepared by UH and HPH methods. The methods require two steps; the first one is common to both procedures and is represented by an emulsification conducted by high-shear mixing. In the second step, the obtained emulsion is treated by two alternative instruments, with the aim to reduce and uniform the droplet size: (a) in the UH method by a probe ultrasound generator and (b) in the HPH method by a high-pressure homogenizer.

The initial emulsion was obtained by dispersing the fused lipids in the aqueous surfactant solution under high speed stirring at 15,000 r.p.m. for 1–3 min. Particle mean diameters, measured by PCS after cooling the emulsion at 25 °C, are reported in Table S 1 (data in brief). Varying the emulsification time (in the 1–3 min range) caused only marginal variations in mean diameter of the obtained particles. Therefore, to shorten the preparation time and save energy in view of an industrial production, the high-shear emulsification step was limited to 1 min.

With respect to the UH step, the influence of the treatment length was investigated on particle size; SLN and NLC dimensions were determined after treatment of 5, 10 and 15 min (Table 1). In further experiments, the UH treatment of 15 min was selected, since it resulted in the production of the smallest nanoparticles (147 and 179 nm for SLN and NLC, respectively).

The effect of length of treatment was evaluated also for the HPH method (i.e. in term number of homogenization cycles). The effect of cycles was investigated on nanoparticle size. As reported in Table 1, mean diameter of SLN and NLC was affected by the number of homogenization cycles. Surprisingly, the smallest dimensions were obtained with a single cycle, therefore in view of scaling up the production procedure, we chose to employ a single homogenization cycle.

For the HPH method, the influence of pressure was also considered. Namely the range 40–120 MPa was investigated (data in brief,

Table 1
Mean diameters of nanoparticles as a function of process parameters.

Process parameters	Z average mean diameter (nm)	
Duration of UH (min)	SLN	NLC
5	200 ± 33	255 ± 45
10	180 ± 28	230 ± 33
15	147 ± 52	179 ± 55
HPH (number of cycles)	SLN	NLC
1	68 ± 15	86 ± 18
2	88 ± 17	102 ± 20
3	99 ± 28	112 ± 14

Data are the mean of 4 determinations in independent experiments.

Fig. S 3); pressure level from 40 to 100 MPa decreased the size, higher pressure levels, up to 120 MPa increased the particle dimension. This behavior was attributed to particle coalescence induced by high kinetic energy of particles. To limit this phenomenon, pressure was set at 100 MPa.

Taken together, the data obtained from the analysis of UH and HPH methods resulted in the selection of the set-up for both methods (Table 2).

3.2. Nanoparticles characterization

The effect of production method and of the presence of PRG has been evaluated with respect to nanoparticle dimensions, presence of agglomerates, EE and LC (Table 3).

Dimensions were measured by PCS and expressed by Z average; data reported in Table 3 indicate that: (a) nanoparticles produced by HPH have consistently smaller dimensions than those produced by UH; indeed, the former are comprised between 68 and 181 nm while the latter span between 125 and 216 nm, (b) Z Average diameters of NLC-PRG are smaller than those of SLN-PRG, particularly in the case of nanoparticles produced by UH and (c) the presence of PRG appears to have an important effect on nanoparticles size; both methods resulted in drug loaded nanoparticle with larger dimensions with respect to the empty counterparts.

Table 2
Experimental set-up for nanoparticle production.

	First step	Second step	
Method		Duration	Energy input
UH	1 min High shear homogenization	15 min	6.75 Hz
HPH	1 min High shear homogenization	1 cycle	100 MPa

Regarding agglomerates, SLN and NLC produced by UH method displayed a presence of 5–8% agglomerate, on the contrary with the HPH method, no agglomerates were detected.

EE and LC values, reported in Table 3, revealed that both methods resulted in high EE (>82%) and LC (>1.64%).

3.3. Morphological analyses of lipid nanoparticles

The morphology of SLN and NLC produced by HPH has been investigated by cryo-TEM and x-ray diffraction. It is important to underline that nanoparticles imaged by cryo-TEM analyses appear different, depending on their orientations. Generally, in the case of top view, both SLN and NLC appear to have a low electron dense discoid structure; while in the case of edge-on view they appear as high electron-dense rod like structures (Fig. 1A and B). This feature is well detectable in the microphotographs relative to the SLN samples (Fig. 1A and C), in which the edge-on viewed nanoparticles have an electron dense rod-shape morphology, without any appreciable structured architecture (at least in the cryo-TEM analysis). On the contrary, NLC display a different internal organization; particularly in the edge-on view, they are characterized by the presence of stacked lamellae capped by semi-elliptical structures (Fig. 1D). Importantly: (a) the presence of the drug does not alter the morphology of both SLN and NLC (see insets in Fig. 1C and D) and (b) the general morphology of nanoparticles produced by HPH is almost identical to that of nanoparticles produced by UH (images not shown) [32].

Nanoparticles produced by HPH have been further characterized by X-ray diffraction analyses. The low-angle region was considered to investigate the structure of SLN, NLC, SLN-PRG and NLC-PRG. The results are reported in Fig. 2, showing that both SLN and NLC display an internal lamellar organization; the calculated unit cell values were 4.52, 4.6, 4.55 or 4.75 nm, for SLN, SLN-PRG, NLC and NLC-PRG respectively. Data indicate that the presence of PRG slightly increased the unit cell dimensions in both type of lipid nanoparticles.

3.4. Stability studies

In view of an industrial application, specific studies have been undertaken on nanoparticles produced by HPH and UH for comparison. Particularly, physico-chemical studies have been conducted, namely to determine the dimension (expressed as Z Average) and the stability of PRG up to 6 months from the production.

The dimensional results show that lipid nanoparticles were well stable in term of size, the formulations produced by both methods maintained their dimensions almost unvaried during the 6 months period analyzed (Fig. 3A and B).

Table 3
Dimensional characteristics, presence of agglomerates and encapsulation parameters of nanoparticles produced by UH or HPH method.

	UH				HPH			
Nanoparticle type	SLN	SLN-PRG	NLC	NLC-PRG	SLN	SLN-PRG	NLC	NLC-PRG
Z average (nm)	147 ± 52	216 ± 22	179 ± 55	125 ± 10	68 ± 15	181 ± 14	86 ± 18	137 ± 18
Dispersity	0.26	0.35	0.27	0.22	0.30	0.31	0.22	0.25
Agglomerate[a] (%)	6 ± 3.5	8 ± 2.2	5 ± 3.8	7 ± 2.3	–	–	–	–
EE[b] (%)	–	82 ± 4	–	88 ± 10	–	97 ± 2	–	99 ± 1
LC[c] (%)	–	1.64	–	1.76	–	1.94	–	1.98

[a] Loss of lipids (lipid phase) due to the partial coalescence of the lipid phase during the formation of the O/W emulsion. After cooling the coalesced lipid phase appeared as a small flake floating on the surface of the NLC dispersion. Data represent the mean ± SD of 6 independent experiments.

[b] Encapsulation efficiency, as defined in Eq. (1).

[c] Loading capacity, as defined in Eq. (2).

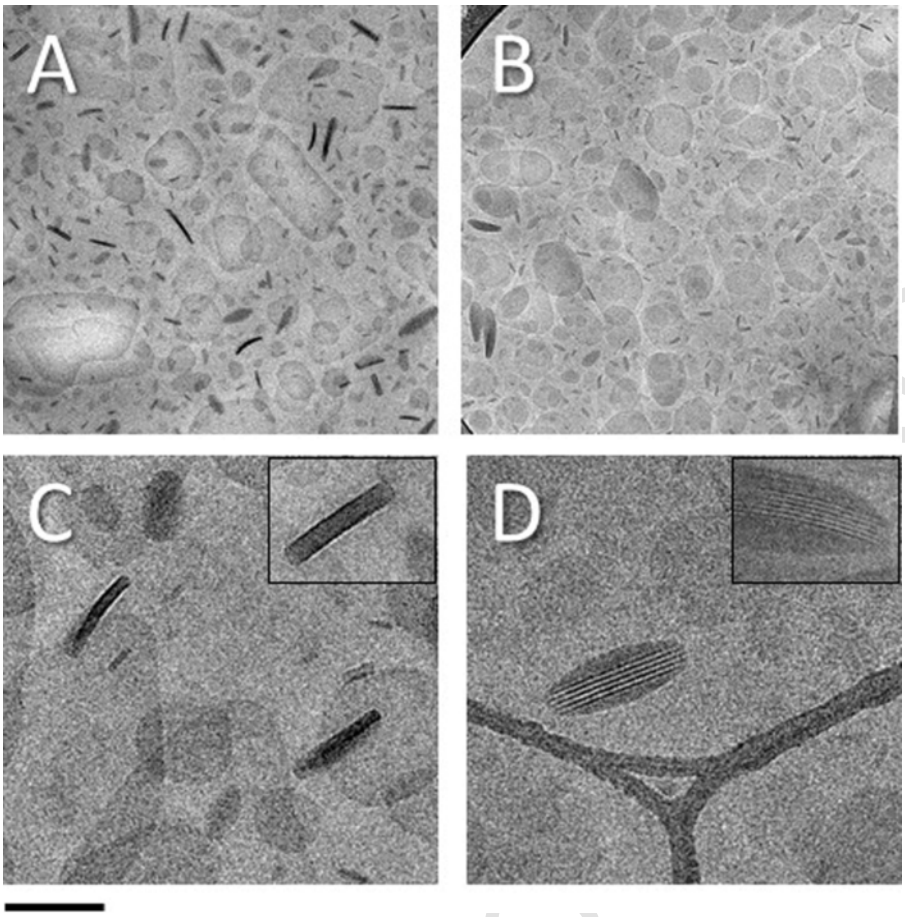

Fig. 1. Cryo-TEM images of SLN-PRG (A, C) and NLC-PRG (B, D) produced by HPH method. For comparison, the insets of panels C and D show microphotographs relative to empty SLN and NLC. Bar corresponds to 300 nm in panels A and B and 150 nm in panels C and D.

To investigate the stability of drug in nanoparticle formulations, PRG content has been determined as a function of time and expressed as percentage with respect to the total amount of drug loaded in the formulation. From the data reported in Fig. 3, it is evident that the drug in NLC-PRG was more stable with respect to that in SLN-PRG. Regarding the production method, nanoparticles produced by HPH (Fig. 3D) were quite more stable than those produced by UH (Fig. 3C). Particularly, PRG residual content after 6 months was 80% and 66%, in the case of NLC-PRG produced by HPH and UH, respectively.

Table 4 reports shelf life (t_{90}) and half-life ($t_{1/2}$) values calculated by Eqs. (4) and (5). The longest shelf life values were found in the case of NLC-PRG produced by HPH. Notably SLN-PRG and NLC-PRG produced by this method displayed t_{90} and $t_{1/2}$ values respectively 3-fold and 2.5-fold longer with respect to nanoparticles produced by UH method.

3.5. In vitro PRG release kinetics

PRG release profiles from nanoparticles produced by HPH were determined in vitro by a dialysis method. Namely SLN-PRG and NLC-PRG were compared; as reference a free drug formulation based on a suspension of the drug in poloxamer 188 (2.5% w/w in water) was taken.

The release of PRG from the different formulations are reported in Fig. 4A. In all cases the obtained profiles are similar in term of general shape. They are characterized by an initial phase in which 50–60% of the PRG is released, afterwards PRG is released much more slowly. In addition, the obtained data indicate that PRG is more slowly released from NLC-PRG.

To determine the mechanism of PRG release form nanoparticles, a mathematical analysis of the release profile was conducted. Theoretical release profiles were calculated according to the linear form of Eqs. (6) and (7), respectively mimicking dissolutive and diffusive model. Then a comparison between the theoretical and experimental release from SLN-PRG (data in brief, Fig. S 4A) and NLC-PRG (data in brief, Fig. S 4B) was performed.

The experimental curve relative to SLN-PRG is almost superimposable to the diffusive theoretical curve [31,33].

Differently, NLC-PRG appear to be dominated by a mixed release mechanism; the experimental curve is indeed partly overlapping the theoretical dissolutive curve and partly the theoretical diffusive curve [22].

3.6. In vitro skin permeability of nanoparticles

In view of vaginal or cutaneous administration of nanoparticles, a thickened formulation would be required since the low viscosity of SLN and NLC aqueous suspensions do not allow the proper application. Therefore, to produce a semisolid formulation containing PRG nanoparticle, the aqueous nanoparticle suspensions were thickened by direct addition of x-gum powder (to a final 1% w/w concentration). X-gum enabled to rapidly obtain gelled formulations, named SLN-PRG/G and NLC-PRG/G.

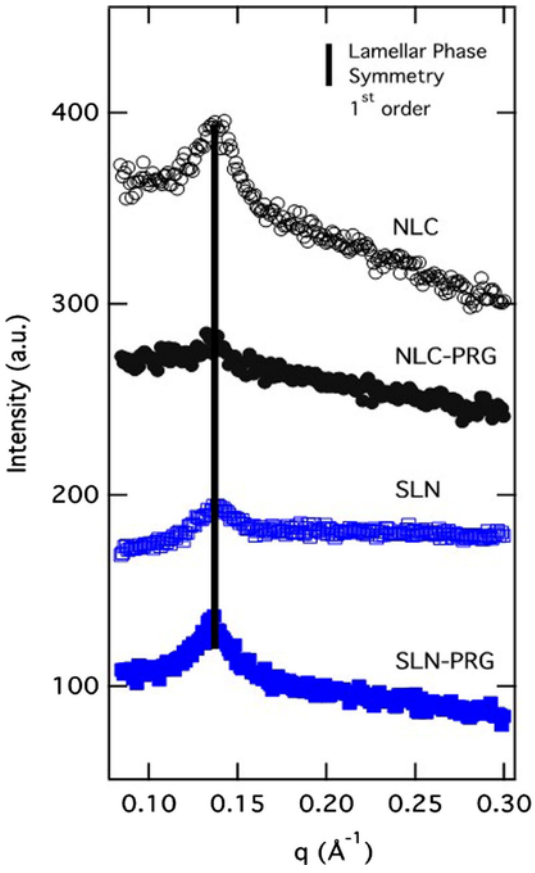

Fig. 2. X-ray diffraction profiles observed for SLN and NLC, in the presence and absence of PRG. From the bottom: SLN-PRG, SLN, NLC-PRG and NLC. The vertical black line indicates the peak position of the first order of the Lamellar Phase Symmetry. Nanoparticles were produced by HPH method.

The skin permeability of PRG included in SLN-PRG/G and NLC-PRG/G was investigated by Franz cell experiments using SCE. To ensure sink condition, a receptor phase constituted of a water/ethanol 1:1 (v/v) mixture was used [25,34]. Drug permeability and skin uptake were evaluated analyzing PRG content in the receptor phase and in the SCE. The results of skin permeability experiments indicate that PRG content in the receptor phase was below the detection limit of the analytical method employed. The analysis of the PRG content in SCE, reported in Fig. 4B, demonstrated that after 6 h similar amounts of PRG were present in the case of SLN-PRG/G and NLC-PRG/G. After 24 h, the presence of PRG in SCE was statistically higher ($p < 0.001$) in the case of SLN-PRG/G with respect to NLC-PRG/G (1.5-fold higher).

3.7. Tape-stripping experiments

After application of nanoparticle formulations on skin, the amount of PRG in *stratum corneum* was assessed by a pilot tape stripping experiment to compare the performances of SLN-PRG/G and NLC-PRG/G [26]. Experiments were carried out as schematized in Fig. 5A–F. Fig. 5G and Table 5 show the amount of PRG present in *stratum corneum* after application of the different formulations and the relative AUC values, respectively. Fig. 5G shows that, at t 1 from removal of the formulations, the amount of PRG in *stratum corneum* was higher for SLN-PRG/G than NLC-PRG/G. The difference in PRG content was confirmed at observation made at t 3 and t 6, as clearly appreciable from the AUC value reported in Table 5. For all the time intervals considered (t 1–3, 3–6 and 1–6), the content of PRG, expressed as AUC, follows the order SLN-PRG/G > NLC-PRG/G. All differences were statistically significative ($p < 0.001$).

Finally, Fig. 5H shows that PRG values at t 3 and t 6 (expressed as percentage of PRG with respect to those found at t 1) display a similar depletion trend.

4. Discussion

Scalability of lipid nanoparticle production from bench to pilot and large scale represents an important challenge in view of industrial production [35]. Since production methods and conditions affect physico-chemical characteristics of the nanoparticles, specific studies are needed to achieve the highest product quality.

In this respect in the current study we have evaluated the effect of HPH process parameters on nanoparticle characteristics, such as size, size distribution and presence of agglomerate.

The performances of HPH were evaluated on the production of SLN and NLC; the obtained data were compared with UH method, a well-known and established process for lipid nanoparticle production [10,17,31]. HPH method enabled to 20-fold increase production volume of nanoparticle with respect to UH. Indeed, by HPH it was possible to obtain 1 l of nanoparticle (amount of lipid 50 g). SLN and NLC produced by HPH have homogeneous size, slightly smaller than those produced by UH, in addition no signs of agglomeration were detectable. Importantly, nanoparticles by HPH resulted in high EE and LC values and were stable, confirming the previously reported results [35]. For instance, PRG encapsulated in lipid nanoparticles produced by HPH was generally stable, even if NLC were able to better control PRG stability with respect to SLN [36].

Dialysis method, performed to mimic subcutaneous administration, indicated that NLC-PRG displayed a slower PRG release (with a combination of dissolutive and diffusive mechanisms) with respect to SLN-PRG, in this latest case a release with a fickian diffusive mechanism was postulated. Franz cell method was performed to mimic cutaneous application. Nevertheless, it should be considered that Franz cell represents an in vitro model which is a reconstruction of the biological environment, mimicking application on SCE membrane, without taking in consideration the full skin and the physiological distribution of PRG through blood capillaries in the dermis [37]. Franz cell study did not evidence PRG content in the receptor phase. This finding corroborates the idea that PRG, being a lipophilic molecule, is strongly associated to the lipid matrix of the nanoparticles. PRG uptake on SCE was higher in the case of SLN-PRG/G with respect to NLC-PRG/G, probably because of a higher affinity and better accommodation of PRG in the liquid phase of NLC [38]. NLC appears as vehicle able to better retain PRG within lipid matrix with respect to SLN.

To overcome the above described limits of the Franz cell method and to investigate more accurately the performances of lipid nanoparticle formulations applied on the skin, in vivo experiments were performed. Tape stripping allowed to directly quantify PRG in the *stratum corneum* after application of the gelled nanoparticle formulations.

PRG depletion effect (i.e. the reduction of PRG content in *stratum corneum* with time) was evident for both nanoparticle type, indicating good transcutaneous penetration. Indeed, it has been reported that lipid nanoparticles applied on skin can interact with *stratum corneum* constituents in reason of their lipophilic molecule composition, nanoscale dimensions and bioadhesive properties [36,39]. The skin absorption of drug delivered by lipid nanoparticle is in addition facilitated by an occlusive effect, skin hydration and a drug penetration

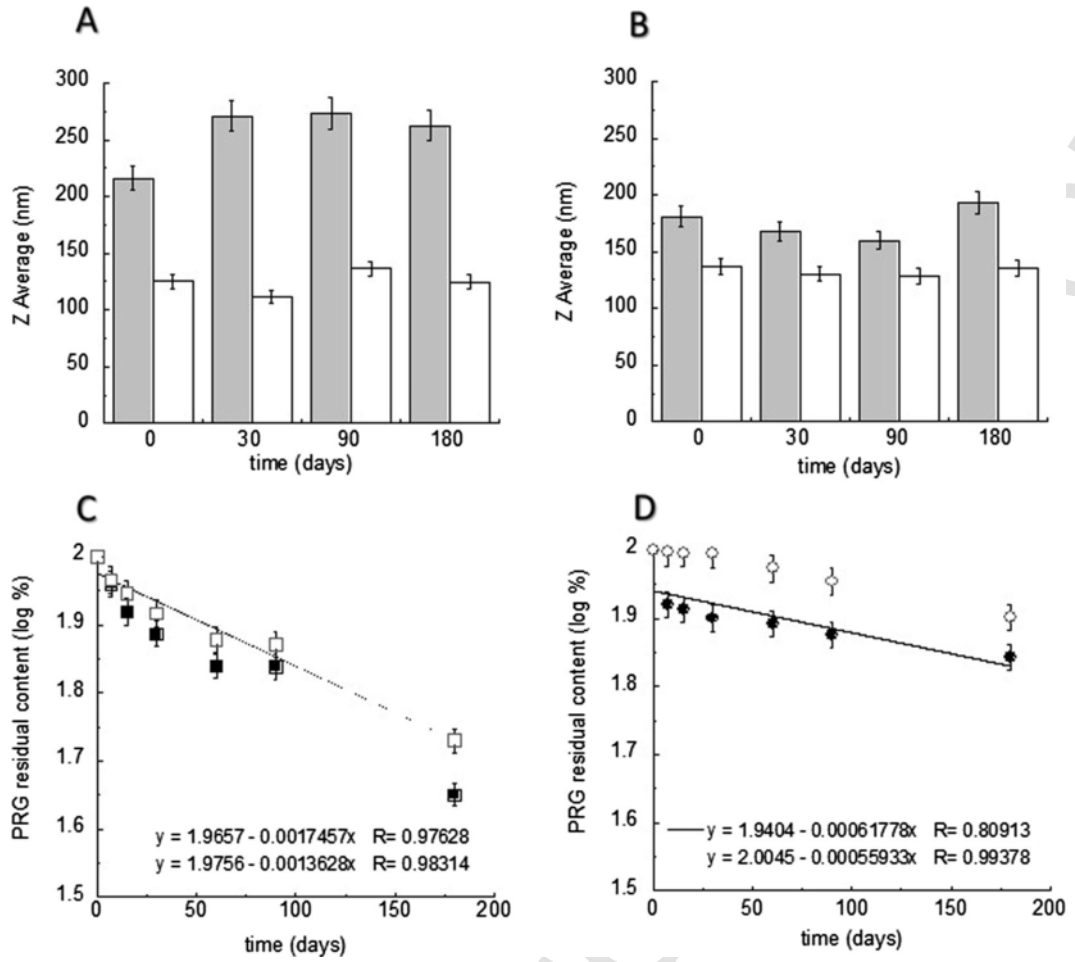

Fig. 3. Effect of aging on Z Average (A, B) and PRG content (C, D) of lipid nanoparticles. SLN-PRG (filled symbols) and NLC-PRG (empty symbols) were produced by UH (A, C) or HPH (B, D) methods. The formulations were stored in glass containers at 25 °C for 3 months. Data are the means of 5 analyses on different batches of the same type of formulations.

Table 4
Shelf life values of nanoparticles produced by UH method or HPH method.

	Nanoparticles produced by UH		Nanoparticles produced by HPH	
Parameter	SLN-PRG	NLC-PRG	SLN-PRG	NLC-PRG
K	0.004	0.0031	0.0014	0.0012
t_{90} (days)[a]	26.11	33.87	73.80	81.51
$t_{1/2}$ (days)[b]	173.25	223.54	495.00	577.50

[a] Time at which the drug concentration has lost 10 % with respect to drug recovery at 0 day.

[b] Time at which the drug concentration has lost 50 % with respect to drug recovery at 0 day. The reported results represent the average of four independent experiments ± S.D.

enhancement due to the components of nanoparticles (i.e. short-medium-chain triglycerides) [10,39,40]. Some authors suggested that nanoparticles smaller than 200 nm form a monolayer on the skin surface, favoring skin moisture, open intercorneocyte spaces and promote drug penetration into deeper layers of the skin, through the transappendageal pathway [41,42]. In this respect, tape stripping experiments indicate that PRG penetrated into *stratum corneum* and deeper skin layers. PRG penetration was slightly higher in the case of SLN-PRG/G, possibly due to a more pronounced occlusive effect induced by the solid nanoparticles [42]. Probably part of nanoparticles remained intact on the skin surface, while another fraction penetrated the *stratum corneum* lipids [25,43,44].

In conclusion, the results presented indicate that both SLN-PRG and NLC-PRG produced by HPH are characterized by a good physical and chemical stability; they are homogeneous and without agglomeration phenomena up to 6 months from the production. Both SLN and NLC display high encapsulation efficiency for PRG, controlling its release and skin uptake. Tape stripping experiments indicate that PRG formulated in SLN/G and NLC/G represent suitable formulations to facilitate and control the skin uptake of the drug. Nevertheless, further in vivo studies are required to better understand the kinetics of PRG distribution in the different skin layers, as well as to evaluate in deeper detail the effect of formulation constituents (i.e. thickening agents and nanoparticle components) on the in vivo performances of lipid nanoparticles.

Acknowledgements

This work was funded by "FIRB 2010. Fondo per gli Investimenti della Ricerca di Base" from the Ministry of the University and Research of Italy (code RBFR10XKHS). The authors are grateful to Prof Carmelo Puglia for providing samples of skin for Franz cell experiments.

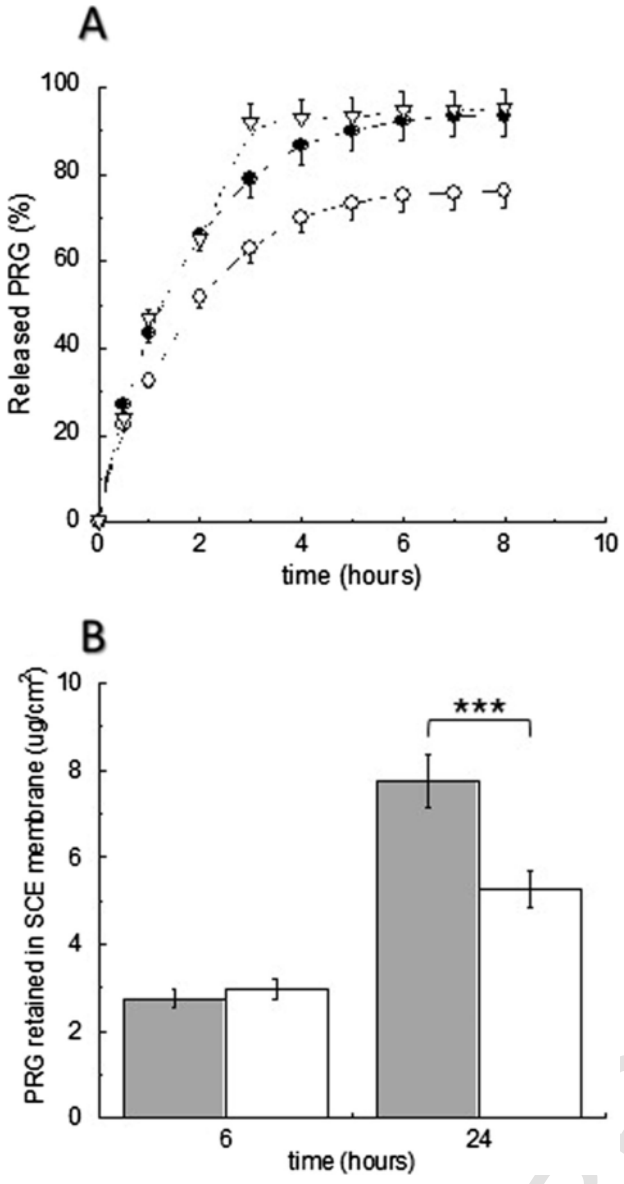

Fig. 4. (A): In vitro release kinetics of PRG from SLN-PRG (●), NLC-PRG (○) and poloxamer 188 suspension (2.5% w/w) (V). Experiments were performed by dialysis method. Data are the mean of 6 experiments ± S.D. (B): PRG skin uptake in SCE membrane from SLN-PRG (filled), NLC-PRG (empty) after 6 and 24 h of permeation experiments in Franz diffusion cells (n = 6); error bars represent the standard deviations; $^{***}p < 0.001$. Nanoparticles were produced by HPH method.

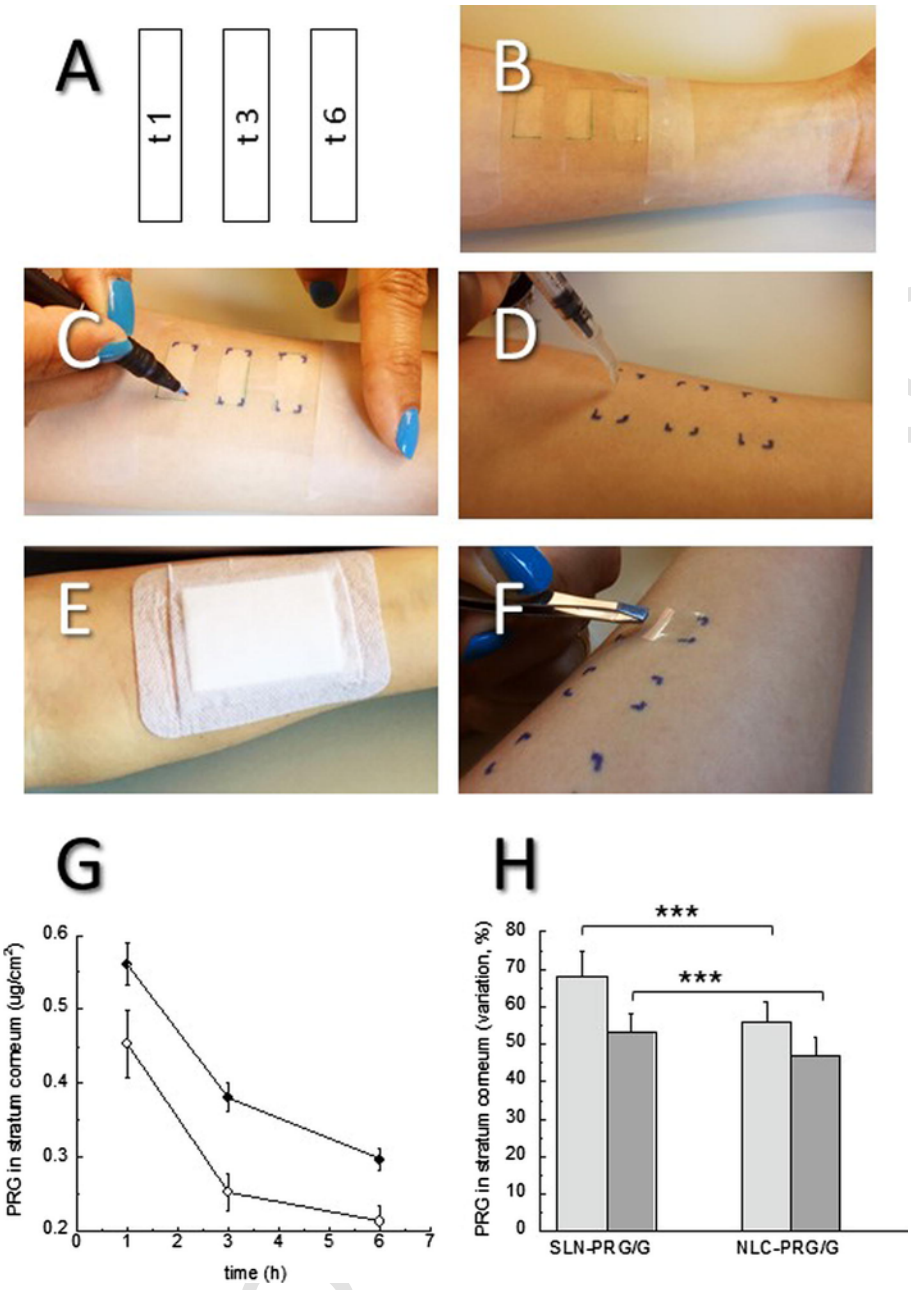

Fig. 5. Tape-stripping experiment on lipid nanoparticle gels. A-F: Time setting (A) and major steps of the tape-stripping experiments; application of a plastic mask on the internal forearm (B), marking of the application sites by permanent ink pen (C), application of the gels by needleless syringe (D), application of backing (E) and removal of stratum corneum layer by tape-stripping (F). Panel G: analysis of PRG amount in *stratum corneum* after application of SLN-PRG/G (●) and NLC-PRG/G (○). Formulations were maintained on the skin for 6 h, thereafter the PRG amount was measured at the indicated lengths of time. Panel H: comparative evaluation of the PRG level present at t 3 (light bars) and t 6 (dark bars) in *stratum corneum*, as determined by tape-stripping experiments. The reported levels represent the percentage of PRG with respect to that present in *stratum corneum* at t 1. Data represent the mean of 10 subjects ± S.D., $^{***}p < 0.001$. Nanoparticles were produced by HPH method.

Table 5
AUC values calculated after tape stripping experiments.

Formulation	AUC t 1–3	AUC t 3–6	AUC t 1–6
SLN-PRG/G	0.94	1.05	1.99
NLC-PRG/G	0.70	0.69	1.39

SLN-PRG/G: solid lipid nanoparticles containing progesterone, thickened by xanthan gum; NLC-PRG/G: nanostructured lipid carriers containing progesterone, thickened by xanthan gum; AUC values were calculated from the plot relative to the amount of PRG in *stratum corneum* versus time (Fig. 5G).

References

[1] M.R. Bhalekar, V. Pokharkar, A. Madgulkar, N. Patil, N. Patil, Preparation and evaluation of miconazole nitrate-loaded solid lipid nanoparticles for topical delivery, AAPS PharmSciTech 10 (2009) 289–296.
[2] G. Abdelbary, R.H. Fahmy, Diazepam-loaded solid lipid nanoparticles: design and characterization, AAPS Pharmscitech 10 (2009) 211–219.
[3] S. Kumar, J.K. Randhawa, High melting lipid based approach for drug delivery: Solid lipid nanoparticles, Mater. Sci. Eng. C 33 (2013) 1842–1852.
[4] E.D.P. Almeida, A.A. Costa, M.R. Serafini, F.C. Rossetti, J.M. Marchetti, V.H.V. Sarmento, A.A.M. Lira, Preparation and characterization of chloroalu-

minum phthalocyanine-loaded solid lipid nanoparticles by thermal analysis and powder X-ray diffraction techniques, J. Therm. Anal. Calorim. 108 (2012) 191–196.
[5] K. Jores, W. Mehnert, M. Drechsler, H. Bunjes, C. Johann, K. Maeder, Investigations on the structure of solid lipid nanoparticles (SLN) and oil-loaded solid lipid nanoparticles by photon correlation spectroscopy, field-flow fractionation and transmission electron microscopy, J. Control. Rel. 95 (2004) 217–227.
[6] V. Jenning, A.F. Thunemann, S.H. Gohla, Characterisation of a novel solid lipid nanoparticle carrier system based on binary mixtures of liquid and solid lipids, Int. J. Pharm. 199 (2000) 167–177.
[7] R.H. Muller, K. Mader, S. Gohla, Solid lipid nanoparticles (SLN) for controlled drug delivery: a review of the state of the art, Eur. J. Pharm. Biopharm. 50 (2000) 161–177.
[8] A. Dingler, S. Gohla, Production of solid lipid nanoparticles (SLN): scaling up feasibilities, J. Microencapsul. 19 (2002) 11–16.
[9] T.G. Leighton, The Acoustic Bubble, Academic press, San Diego, 1994.
[10] M. Uner, Preparation, characterization and physico-chemical properties of Solid Lipid Nanoparticles (SLN) and Nanostructured Lipid Carriers (NLC): Their benefits as colloidal drug carrier systems, Pharmazie 61 (2006) 375–386.
[11] S. Das, A. Chaudhury, Recent advances in lipid nanoparticle formulations with solid matrix for oral drug delivery, AAPS PharmSciTech 12 (2011) 62–76.
[12] G. Lockwood, G. Griesinger, B. Cometti, Subcutaneous progesterone versus vaginal progesterone gel for luteal phase support in in vitro fertilization: a noninferiority randomized controlled study, Fertil. Steril. 101 (2014) 112–119.
[13] A. Tavaniotou, J. Smitz, C. Bourgain, P. Devroey, Comparison between different routes of progesterone administration as luteal phase support in infertility treatments, European Centers, Hum. Reprod. Update 6 (2000) 139–148.
[14] K.A. Burry, P.E. Patton, K. Hermsmeyer, Percutaneous absorption of progesterone in postmenopausal women treated with transdermal estrogen, Am. J. Obstet. Gynecol. 180 (1999) 1504–1511.
[15] G. Holzer, E. Riegler, H. Hönigsmann, S. Farokhnia, J.B. Schmidt, Effects and side-effects of 2% progesterone cream on the skin of peri- and postmenopausal women: results from a double-blind, vehicle-controlled, randomized study, Br. J. Dermatol. 153 (2005) 626–634.
[16] R. Pecora, Dynamic Light Scattering Measurement of Nanometer Particles in Liquids, J. Nanoparticle Res. 2 (2000) 123–131.
[17] E. Esposito, M. Fantin, M. Marti, M. Drechsler, L. Paccamiccio, P. Mariani, E. Sivieri, F. Lain, E. Menegatti, M. Morari, R. Cortesi, Solid lipid nanoparticles as delivery systems for bromocriptine, Pharm. Res. 25 (2008) 1521–1530.
[18] V. Luzzati, H. Delacroix, T. Gulik-Krzywicki, P. Mariani, R. Vargas, The cubic phases of lipids, Curr. Top. Membr. 44 (1997) 3–24.
[19] C. Puglia, V. Cardile, A.M. Panico, L. Crascì, A. Offerta, S. Caggia, M. Drechsler, P. Mariani, R. Cortesi, E. Esposito, Evaluation of monooleine aqueous dispersions as tools for topical administration of curcumin: characterization, in vitro and ex-vivo studies, J. Pharm. Sci. 102 (2013) 2349–2361.
[20] W.J. Pugh, Kinetics of product stability, in Aultons's Pharmaceutics, M.E. Aulton (Ed.), The design and manufacture of the medicines, Churchil Livingstone Elsevier, London, 2007, pp. 99–107.
[21] N.A. Peppas, Analysis of Fickian and non-Fickian drug release from polymers, Pharm. Acta Helv. 60 (1985) 110–111.
[22] J. Siepmann, F. Siepmann, Mathematical modeling of drug delivery, Int. J. Pharm. 364 (2008) 328–343.
[23] C. Puglia, F. Bonina, L. Rizza, R. Cortesi, E. Merlotti, M. Drechsler, P. Mariani, C. Contado, L. Ravani, E. Esposito, Evaluation of percutaneous absorption of naproxen from different liposomal formulations, J. Pharm. Sci. 99 (2010) 2819–2829.
[24] M. Siewert, J. Dressman, C.K. Brown, V.P. Shah, FIP/AAPS guidelines to dissolution/in vitro release testing of novel/special dosage forms, AAPS PharmSciTech 4 (2003) E7.
[25] L.M. Andrade, C. de Fátima Reis, L. Maione-Silva, J.L.V. Anjos, A. Alonso, R.l.C. Serpa, R.N. Marreto, E.M. Lima, S.F. Taveira, Impact of lipid dynamic behavior on physical stability, in vitro release and skin permeation of genistein-loaded lipid nanoparticles, Eur. J. Pharm. Biopharm. 88 (2014) 40–47.
[26] E. Esposito, L. Ravani, P. Mariani, N. Huang, P. Boldrini, M. Drechsler, G. Valacchi, R. Cortesi, C. Puglia, Effect of nanostructured lipid vehicles on percutaneous absorption of curcumin, Eur. J. Pharm. Biopharm. 86 (2014) 131–132.
[27] H. Yuan, L.-L. Wang, Y.-Z. Du, J. You, F.-Q. Hu, S. Zeng, Preparation and characteristics of nanostructured lipid carriers for control-releasing progesterone by melt-emulsification, Colloids Surf. B Biointerfaces 60 (2007) 174–179.
[28] D. Pooja, L. Tunki, H. Kulharia, B.B. Reddy, R. Sistla, Characterization, biorecognitive activity and stability of WGA grafted lipid nanostructures for the controlled delivery of Rifampicin, Chem. Phys. Lipids 193 (2015) 11–17.
[29] E. Esposito, A. Boschi, L. Ravani, R. Cortesi, M. Drechsler, P. Mariani, S. Moscatelli, C. Contado, G. Di Domenico, C. Nastruzzi, M. Giganti, L. Uccelli, Biodistribution of nanostructured lipid carriers: a tomographic study, Eur. J. Pharm. Biopharm. 89 (2015) 145–156.
[30] E. Esposito, M. Drechsler, R. Cortesi, C. Nastruzzi, Encapsulation of cannabinoid drugs in nanostructured lipid carriers, Eur. J. Pharm. Biopharm. 102 (2016) 87–91.
[31] E. Esposito, R. Cortesi, M. Drechsler, J. Fan, B.M. Fu, L. Calderan, S. Mannucci, F. Boschi, C. Nastruzzi, Nanoformulations for dimethyl fumarate: physicochemical characterization and in vitro/in vivo behavior, Eur. J. Pharm. Biopharm. 115 (2017) 285–296.
[32] E. Esposito, M. Drechsler, P. Mariani, F. Carducci, M. Servadio, F. Melancia, P. Ratano, P. Campolongo, V. Trezza, R. Cortesi, C. Nastruzzi, Lipid nanoparticles for administration of poorly water soluble neuroactive drugs, Biomed. Microdevices 19 (2017) 44–58.
[33] L.C. Herrera, M.V. Defain Tesoriero, L.G. Hermida, In vitro release testing of PLGA microspheres with franz diffusion cells, Dissolution Technol. 5 (2012) 6–11.
[34] E. Toitou, B. Fabin, Altered skin permeation of highly lipophilic molecule: Tetrahydrocannabinol, Int. J. Pharm. 43 (1988) 17–22.
[35] R. Paliwal, R. Jayachandra Babu, S. Palakurthi, Nanomedicine scale-up technologies: feasibilities and challenges, AAPS PharmSciTech 15 (2014) 1527–1534.
[36] J. Pardeike, A. Hommoss, R.H. Müller, Lipid nanoparticles (SLN, NLC) in cosmetic and pharmaceutical dermal products, Int. J. Pharm. 366 (2009) 170–184.
[37] Y. Hazama, T. Maekawa, R. Miki, S. Oshima, Y. Egawa, K. Morimoto, T. Seki, Effect of physiological changes in the skin on systemic absorption of tacrolimus following topical application in rats, Biol. Pharm. Bull. 39 (2016) 343–352.
[38] S. Küchler, M.R. Radowski, T. Blaschke, M. Dathe, J. Plendl, R. Haag, M. Schäfer-Korting, K.D. Kramer, Nanoparticles for skin penetration enhancement–a comparison of a dendritic core-multishell-nanotransporter and solid lipid nanoparticles, Eur. J. Pharm. Biopharm. 71 (2009) 243–250.
[39] S.A. Wissing, A. Lippacher, R.H. Muller, Investigations on the occlusive properties of solid lipid nanoparticles (SLN), J. Cosmet. Sci. 52 (2001) 313–324.
[40] A. Lippacher, R.H. Müller, K. Mäder, Semi-solid SLN$^{(TM)}$ dispersions for topical application: Influence of formulation and production parameters on viscoelastic properties, Eur. J. Pharm. Biopharm. 53 (2002) 155–160.
[41] S.A. Wissing, R.H. Müller, The influence of solid lipid nanoparticles on skin hydration and viscoelasticity—in vivo study, Eur. J. Pharm. Biopharm. 56 (2003) 67–72.
[42] M. Üner, G. Yener, Importance of solid lipid nanoparticles (SLN) in various administration routes and future perspectives, Int. J. Nanomed. 2 (2007) 289–300.
[43] V. Teeranachaideekul, E.B. Souto, R.H. Müller, V.B. Junyaprasert, Physicochemical characterization and in vitro release studies of ascorbyl palmitate-loaded semi-solid nanostructured lipid carriers (NLC gels), J. Microencapsul. 25 (2008) 111–120.
[44] S. Khurana, P.M.S. Bedi, N.K. Jain, Preparation and evaluation of solid lipid nanoparticles based nanogel for dermal delivery of meloxican, Chem. Phys. Lipids 175–176 (2013) 65–72.